Spatial and temporal pattern of human activity intensity and its driving mechanism in the Turpan- Hami Basin, China from 1990 to 2020 Postprint

Authors: SHI Qingqing

Date: 2025-11-14T00:00:00+00:00

Abstract

The Turpan-Hami (Tuha) Basin of China, a critical region on the Silk Road Economic Belt and a major national energy base, occupies a significant position in energy security and in the major industrial clusters in Xinjiang Uygur Autonomous Region, China. Understanding spatial and temporal evolution of human activities in this area is essential for harmonizing ecological protection with energy development, safeguarding the ecological security of the Silk Road Economic Belt, and promoting the sustainable development of the area. However, despite rapid socioeconomic advances, the trajectories of human activity intensity and the principal driving mechanisms over the past three decades remain inadequately understood. To address these gaps, this study constructed a land use dataset for the Tuha Basin from 1990 to 2020, utilizing Google Earth Engine (GEE) and random forest classification algorithm. We assessed the intensity of human activities and their spatial autocorrelation patterns and further identified key drivers influencing spatial and temporal variations using the Geodetector model. Our findings indicated that the intensity of human activities in the Tuha Basin has exhibited a "first decline and then recovery" trend over the past 30 a, accompanied by significant spatial clustering. In recent years, the aggregation of hot spots has diminished, while clustering of cold spots has intensified, suggesting a dispersion of human activity centers. Nevertheless, urban areas in the Hami and Turpan cities, along with their surrounding areas, continued to serve as core areas of human activities. Topographic features (slope gradient and aspect) and their interactions with economic variables emerged as dominant determinants shaping the spatial patterns and temporal dynamics of human activity intensity. This result provides critical insights into fostering sustainable regional development and ecological conservation in the Tuha Basin and offers valuable methodological and empirical references for studies on land

use dynamics and human activity intensity in similar arid areas.

Full Text

Preamble

J Arid Land (2025) 17(11): 1497–1517
doi: 10.1007/s40333-025-0032-8; CSTR: 32276.14.JAL.02500328
Science Press Springer-Verlag

Spatial and temporal pattern of human activity intensity and its driving mechanism in the Turpan-Hami Basin, China from 1990 to 2020

SHI Qingqing[1], YIN Benfeng[2], HUANG Jixia[1,3], YIN Yuanyuan[4,5*], YANG Ao[2], ZHANG Yuanming[2]

[1] State Key Laboratory of Efficient Production of Forest Resources, Beijing Forestry University, Beijing 100083, China
[2] State Key Laboratory of Ecological Safety and Sustainable Development in Arid Lands, Xinjiang Institute of Ecology and Geography, Chinese Academy of Sciences, Urumqi 830011, China
[3] Academy of Plateau Science and Sustainability, People' s Government of Qinghai Province & Beijing Normal University, Xining 810008, China
[4] Institute of Science and Technology Education, Beijing Union University, Beijing 100011, China

Abstract

The Turpan-Hami (Tuha) Basin of China, a critical region on the Silk Road Economic Belt and a major national energy base, occupies a significant position in energy security and in the major industrial clusters in Xinjiang Uygur Autonomous Region, China. Understanding the spatial and temporal evolution of human activities in this area is essential for harmonizing ecological protection with energy development, safeguarding the ecological security of the Silk Road Economic Belt, and promoting sustainable development. However, despite rapid socioeconomic advances, the trajectories of human activity intensity and the principal driving mechanisms over the past three decades remain inadequately understood. To address these gaps, this study constructed a land use dataset for the Tuha Basin from 1990 to 2020, utilizing Google Earth Engine (GEE) and a random forest classification algorithm. We assessed the intensity of human activities and their spatial autocorrelation patterns and further identified key drivers influencing spatial and temporal variations using the Geodetector model. Our findings indicated that the intensity of human activities in the Tuha Basin has exhibited a "first decline and then recovery" trend over the past 30 years, accompanied by significant spatial clustering. In recent years, the aggregation of hot spots has diminished, while clustering of cold spots has intensified, suggesting a dispersion of human activity centers. Nevertheless, urban

areas in the Hami and Turpan cities, along with their surrounding areas, continued to serve as core areas of human activities. Topographic features (slope gradient and aspect) and their interactions with economic variables emerged as dominant determinants shaping the spatial patterns and temporal dynamics of human activity intensity. This result provides critical insights into fostering sustainable regional development and ecological conservation in the Tuha Basin and offers valuable methodological and empirical references for studies on land use dynamics and human activity intensity in similar arid areas.

Keywords: Turpan-Hami Basin; land use change; Google Earth Engine; human activity intensity; interaction

Citation: SHI Qingqing, YIN Benfeng, HUANG Jixia, YIN Yuanyuan, YANG Ao, ZHANG Yuanming. 2025. Spatial and temporal pattern of human activity intensity and its driving mechanism in the Turpan-Hami Basin, China from 1990 to 2020. *Journal of Arid Land*, 17(11): 1497–1517. https://doi.org/10.1007/s40333-025-0032-8; https://cstr.cn/32276.14.JAL.02500328

Corresponding author: YIN Yuanyuan (E-mail: sftyuanyuan@buu.edu.cn)
Received 2025-05-14; revised 2025-08-17; accepted 2025-09-08

http://jal.xjegi.com; www.springer.com/40333

1 Introduction

The intensity of human activities refers to the degree of disturbance and impact exerted on ecosystems at a given spatial scale [**?**]. It reflects the extent of human influence and transformation of the natural environment across different spatial and temporal scales, encompassing a wide range of activities such as urbanization, agricultural reclamation, and industrialization. In the context of globalization and accelerated urbanization, the demand for natural resources has intensified, leading to significant changes in land use and ecological environment. These changes have triggered a series of ecological and environmental problems, including land degradation [**?**], species extinction, and climate change [**?**]. Quantitative evaluation of human activity intensity is crucial for better understanding and predicting the impacts of human activities on regional ecosystems, which provides a scientific basis for ecological protection, rational resource allocation, and promotion of sustainable development.

The intensity of human activities is a critical indicator of the impact of socio-economic activities on natural ecosystems. Methods for measuring this intensity are generally divided into two main categories: multi-factors integrated evaluation methods and land use type evaluation methods. Among the multi-factors integrated evaluation methods, the human footprint index method is widely used

[?, ?, ?, ?]. This method integrates a variety of variables, such as population density, nighttime lighting, and human-made surfaces [?, ?, ?], and combines expert scoring method, entropy method, and other methods to determine the indicator weights [?], ultimately generating a weighted sum to assess human activity intensity. Although this method offers strong spatial directionality, it involves a certain degree of subjectivity in indicator selection and weight assignment, which may introduce bias into the results. In contrast, the land use type evaluation method assesses human activities based on changes in land use types and reflects the degree of human influence on surface ecology through the extent of utilization across different land categories. This approach has clear physical significance and strong spatial and temporal comparability, and yields highly accurate measurement results [?, ?, ?]. In recent years, domestic research has further refined this method by integrating high-precision remote sensing data and detailed land classification standards, thereby constructing comprehensive evaluation systems suited to areas lacking statistical data and significantly improving the method' s applicability and universality [?].

Spatial and temporal variation of human activity intensity is jointly influenced by a variety of natural and anthropogenic factors, characterized by multi-dimensional and multi-scale mechanisms. Population growth and distribution are primary drivers that directly influence the intensity of human activities. In densely populated areas, the growing demand for resources, accelerated infrastructure development, and diversified lifestyles collectively drive higher activity intensities. For instance, a significant and positive correlation between population density and human activity intensity is observed along the eastern coast of China [?]. Furthermore, the level of economic development is a key factor shaping the intensity of human activities. Industrialization and urbanization processes have accelerated natural resource exploitation. For example, urbanization and transportation conditions have a significantly positive impact on the intensity of human activities on the Qinghai-Xizang Plateau, China [?]. Natural environmental conditions also play a critical role. Topography, for instance, restricts land availability and thus influences development intensity. The relatively flat southeastern Loess Plateau has become a high-intensity human activity area, whereas the hilly northwestern areas experience lower activity intensity due to topographical constraints [?]. In arid areas, water resource distribution is the dominant factor, which is directly regulated by oasis water management, the expansion of farmland, and the contraction of watersheds in arid oasis ecosystems [?]. Overall, demographic, economic, and environmental factors interactively shape the spatial and temporal distribution of human activity intensity. Therefore, a comprehensive understanding of these interactions is essential when examining the driving mechanisms behind human activity intensity.

In arid areas of China, the intensity of human activities and land use changes show significant geographic variability [?, ?]. Different arid areas exhibit different evolutionary trajectories of land use structure and human activity intensity due to differences in water resource conditions, topography, and policy orienta-

tion. For example, the peripheral area of the Tarim Basin is dominated by oasis agricultural expansion, with a significant increase in cropland and built-up land, while the central desert area has less change and a lower overall intensity of human activities [**?**, **?**]; and the proportion of its industrial land use due to salt lake resource development and energy extraction is rising in the Qaidam Basin [**?**, **?**]. In contrast, human activity characteristics of the Tuha Basin, which is a key node of the Silk Road Economic Belt and an important bridge between Central and East Asia, are more complex [**?**, **?**]. This basin has multiple geographic units such as agricultural and pastoral intertwined areas, resource extraction areas, and oasis economic areas. The basin is renowned for its abundant production of grapes and cantaloupes, forming one of three major special forest and fruit belts in Xinjiang Uygur Autonomous Region, China [**?**]. At the same time, the basin is rich in oil and gas resources and possesses coal reserves exceeding one trillion tons, making it a vital energy base for China [**?**, **?**]. Since the mid-20th century, frequent and intensified human activities have significantly altered the spatial structure of human habitation areas within the basin. However, research on the spatial and temporal evolution of human activity intensity and its driving mechanisms in this basin remains limited. In particular, it is crucial to address the scientific question of how to accurately quantify the spatial and temporal variations in human activity intensity in the Tuha Basin and identify the dominant driving factors, in order to achieve a harmonious balance between regional economic development and ecological conservation. Answering this question is essential for formulating effective ecological protection strategies, optimizing resource management practices, and promoting sustainable regional development.

Therefore, this study focused on the Tuha Basin, constructing a land use classification dataset based on field-collected sample points and Landsat imagery. By calculating human activity intensity indices at multiple spatial scales, the study analyzed the evolution of spatial and temporal patterns and investigated the underlying driving mechanisms. The findings aim to provide critical references for regional ecological protection, resource management, and policy formulation, ultimately supporting the coordinated development of economic growth and ecological sustainability in the Tuha Basin.

2.1 Study Area

The Tuha Basin, also referred to as the Turpan-Hami Basin, is located in eastern Xinjiang Uygur Autonomous Region, China (40°49 -45°03 N, 87°44 -96°25 E; Fig. 1 [FIGURE:1]). The basin stretches approximately 660 km from east to west and spans 60–100 km from north to south, covering a total area of about 53.50$\times 10\hat{}\{3\}$ km^2. The basin is characterized by low elevation and gentle terrain. The basin exhibits a typical continental arid climate, marked by extremely high temperatures in summer, severe cold in winter, and scarce annual precipitation.

2.2 Dataset

The data used in this study comprised five categories: satellite images, field sample points, elevation, climatic data, and socio-economic data (Table 1).

2.2.1 Satellite Images

Given the satellite operation periods and the spectral bands of different Landsat sensors, we obtained satellite images from the publicly accessible Google Earth Engine (GEE) data in 2020, Landsat 8 Operational Land Imager (OLI) sensor in 2015, and Landsat 5 Thematic Mapper (TM) sensor in 1990, 1995, 2000, 2005, and 2010. Since vegetation varies across seasons, we selected remote sensing images from May to September in each year to ensure classification accuracy. These images were cloud-free and underwent atmospheric correction. To represent the data for each year, we computed the average of images collected from May to September.

2.2.2 Sample Point Data

The sample point data consisted of field-collected and visually interpreted sample points. Two field surveys were conducted in the Tuha Basin: one from 1–5 May 2023, and the other from 20 June–10 July 2023. These surveys aimed to investigate land use types based on the region' s ecosystem, human activity intensity, and road accessibility. To ensure the representativeness of samples, we conducted two field surveys along all the main roads in the Tuha Basin and selected the sample points randomly and evenly. During the surveys, typical land use types were photographed at both the hinterland and cross-sections. For each land use type, points were recorded at 30 km intervals, resulting in a total of 234 sample points. To supplement the limited number of field-collected sample points, we interpreted an additional 247 sample points visually using Google Earth imagery.

2.2.3 Elevation Data

The elevation data in 2015, provided by the European Space Agency, has a resolution of 30.00 m. Slope and aspect, which are essential factors in analysis of the changes in human activity intensity, were calculated from the elevation data.

2.2.4 Climate Data

The climate data included monthly temperature and precipitation, provided by the National Earth System Science Data Center (http://www.geodata.cn/oldindex.html) at a resolution of 1000.00 m. We calculated multi-year averages for the years 1990, 1995, 2000, 2005, 2010, 2015, and 2020.

2.2.5 Socio-economic Data

The socio-economic data included gross domestic product (GDP), total agricultural output, and population for each county. GDP and agricultural output data were obtained from the Xinjiang Statistical Yearbook, while population was sourced from the Resource and Environmental Science Data Platform (https://www.resdc.cn/Default.aspx), with a spatial resolution of 1000.00 m. Data for all three indicators were compiled for the years 1990, 1995, 2000, 2005, 2010, 2015, and 2020.

2.3 Methods

This study focused on the following aspects: the construction and accuracy verification of a land use dataset based on random forest, the calculation of human activity intensity, the analysis of spatial pattern, and the investigation of driving mechanisms behind the evolution of spatial and temporal patterns of human activity intensity. The research framework is illustrated in Figure 2 [FIGURE:2].

2.3.1 Land Use Classification

Forest land, water body, desert, urban land, farmland, and bare land in the Tuha Basin were classified [**?**]. The following five feature variables were selected to enhance the classification accuracy and robustness of land cover: Normalized Difference Vegetation Index (NDVI), New Water Index (NWI), Enhanced Water Index (EWI) [**?**], Normalized Difference Bare Land and Built-up Index (NDBBI) [**?**], and Normalized Difference Impervious Surface Index (NDISI).

A random forest model was employed to construct the land use dataset for the Tuha Basin. To address the limited number of sample points for land use types, we conducted supplementary sampling through visual interpretation of high-resolution Google Earth images (0.27 m spatial resolution). About 476 sample points were used for supervised classification, with 128 in forest land, 56 in urban land, 187 in desert, 20 in water body, 51 in farmland, and 34 in bare land (Fig. 1). Of these sample points, 70.00% were used for training and 30.00% for accuracy assessment.

To ensure the accuracy and reliability of the classification results, we used the confusion matrix assessment method [**?**, **?**] and Kappa coefficient (K). We also compared the land-use dataset with the China Land Cover Dataset (CLCD) and the GLC_{FCS30D} dataset (the first global fine land cover dynamic product at a 30.00-m resolution). The CLCD, based on Landsat imagery on GEE, provides annual data at a 30.00-m resolution from 1985 to 2022 [**?**], while the GLC_{FCS30D} dataset, utilizing continuous change detection technology, spans from 1985 to 2022 and includes 35 land-cover categories [**?**]. To ensure the comparability of the datasets, we utilized the vector boundaries of the Tuha Basin and clipped and reclassified the original CLCD dataset and

GLC_{FCS30D} dataset to standardize the classification system (Fig. S1; Tables S1 and S2).

2.3.2 Calculation of Human Activity Intensity

Human activity intensity of land surface (HAILS) is a comprehensive indicator that characterizes the extent of human impact and influence on the land surface [**?**], and is calculated using the following formulas:

$$\mathrm{HAILS} = \frac{\mathrm{SCLE}}{S} \times 100\%$$

$$\mathrm{SCLE} = \sum_{i=1}^{n} (\mathrm{SL}_i \times \mathrm{CI}_i)$$

where SCLE is the equivalent area of urban land (km^2); S is the area of all land use types (km^2); n is the number of land use/land cover types in the basin; SL is the area of the ith land use/land cover type (km^2); and CI is the equivalent conversion coefficient of urban land for the ith land use/land cover type. The urban land equivalent conversion coefficient of land use types in this study adopted the factor system proposed by Xu et al. (2016). This system is based on the systematic judgment of human intervention characteristics of land use/cover types, combined with the expert scoring method and field survey verification, reflecting specific intervention intensity of different land types in "use-transformation-development." In this study, original coefficient values of desert (0.00), bare land (0.00), water body (0.60), urban land (1.00), and farmland (0.20) were used, and the average of different forest land coefficients in the literature was taken as the forest land coefficient (0.11) [**?**].

2.3.3 Spatial Autocorrelation

Moran' s I index is a statistic used to measure spatial autocorrelation, reflecting the presence or absence of structured correlation in the spatial distribution of a variable [**?**, **?**]. Its purpose is to assess the degree of spatial similarity, i.e., whether data values in a spatial area exhibit similar (or dissimilar) characteristics to values in its neighboring areas. In this study, the Moran' s I index was used to reflect the degree of similarity in the intensity of human activities in spatial neighborhoods or spatial proximity, which was calculated using the following formula:

$$I = \frac{N}{W} \frac{\sum_{i=1}^{N} \sum_{j=1}^{N} w_{ij}(z_i - \bar{z})(z_j - \bar{z})}{\sum_{i=1}^{N} (z_i - \bar{z})^2}$$

where z and z are the intensity of human activities in areas i and j, respectively (%); w is the degree of influence between spatial units i and j; and $\bar{z}$ is the

mean value of the intensity of human activities in the whole Tuha Basin (%). The range of Moran' s I index is between -1.00 and 1.00. Moran' s I > 0.00 indicates positive spatial correlation, and the larger the value, the more obvious the spatial correlation; Moran' s I < 0.00 indicates negative spatial correlation, and the smaller the value, the larger the spatial difference; and Moran's I = 0.00 indicates spatial stochasticity. The significance of Moran' s I was assessed using the standardized Z score, which indicates whether the clustering or dispersion could be the result of random chance or is statistically significant.

In this study, hotspot analysis was used to reveal the degree of spatial agglomeration or sparseness of the population and to identify densely or sparsely populated areas [**?**]. This analysis was carried out with the help of the Getis-Ord Gi* module under the geographic information system (GIS) software, and the calculation formula is as follows:

$$G_i^* = \frac{\sum_{j=1}^{N} w_{ij}x_j - \bar{X}\sum_{j=1}^{N} w_{ij}}{S\sqrt{\frac{N\sum_{j=1}^{N} w_{ij}^2 - (\sum_{j=1}^{N} w_{ij})^2}{N-1}}}$$

where w is the spatial weight between feature i and j; x is the attribute value for feature j; $\bar{X}$ is the mean of the variable; and S is the standard deviation of the observation of variable.

2.3.4 Geodetector

The Geodetector was employed to quantify the degree of influence of various factors on the temporal pattern of anthropogenic intensity [**?**]. Human activity intensity was considered the dependent variable. The independent variables included precipitation, temperature, elevation, slope, slope direction, population, GDP, and agricultural output. In this study, factor detection was used to analyze the individual influences on the temporal pattern of human activity intensity, while interaction detection was applied to examine the combined effects of pairs of factors.

Factor detection calculates the degree of influence of different factors on land use change in the Tuha Basin. The q-value is used to represent the magnitude of this influence, where the range of q is between 0.00 and 1.00. A q-value closer to 1.00 indicates a stronger influence of the factor on land use change. The calculation formula is as follows:

$$q = 1 - \frac{\sum_{h=1}^{L} N_h \sigma_h^2}{N\sigma^2} = 1 - \frac{\mathrm{SSW}}{\mathrm{SST}}$$

where h is the stratum index used to identify different categories or partitions (h = 1, 2, 3, ···, L); L is the stratification of land use degree or each influencing factor; N and N are the number of units in stratum h and the whole area,

respectively; σ^{2} and σ^2 are the variance of land use degree in stratum h and the whole area, respectively; SSW is the sum of variance of each category; and SST is the variance of the whole area.

Interaction detection, by identifying the interaction between two driving factors, i.e., X_1 and X_2, can evaluate whether the two factors together strengthen or weaken the effect of a single factor, or whether these driving factors can play a role in independently influencing land-use change [**?**], and the types of interactions are shown in Table 2 .

3.1 Accuracy of Land Use Classification

The land use classification of the Tuha Basin, based on the random forest algorithm, is effective. The average overall accuracy was 0.82, with all values exceeding 0.73. Notably, the overall accuracy reached 0.92 in 2020 (Table 3). The average K value for the classification was 0.75, with all values above 0.64, and the K value in 2020 was 0.89. The ranges of $0.60 \leq K < 0.80$ and $0.80 \leq K < 1.00$ indicated substantial agreement and near perfect agreement, respectively. The results showed good consistency between the classified images and the reference images of the sample points. Therefore, the random forest model had a high degree of accuracy in identifying the type of land uses.

3.2 Land Use Dynamics

From 1990 to 2020, the dominant land use type in the Tuha Basin was desert, which showed an increasing trend, whereas the proportions of other land use types, such as forest land, water body, and farmland, declined. The largest proportion (larger than 87.00%) of land use of the Tuha Basin was desert with an area of 335,290.42 km^2 in 1990, and increased to 350,859.67 km^2 (91.42%) in 2020 (Table 4). In contrast, the smallest proportion (less than 1.00%) of land use is the water body, peaking at 0.76% in 2000. The proportion of forest land was 1.74% in 1990, but decreased steadily, reaching its lowest value (0.79%) in 2015. However, it slightly recovered to 1.20% in 2020. Urban land fluctuated slightly, typically ranging between 2.00% and 3.00%, with a slight decrease from 3.29% in 1990 to 3.24% in 2020. Farmland reached its highest proportion in 1995 (4.58%), but gradually declined to 2.34% in 2020. The proportion of bare land fluctuated, from 4.12% in 1990 to 2.43% in 1995, and then slightly increased to 1.55% in 2020.

Over the past 30 years, the Tuha Basin presented frequent land-use conversion, with a general trend toward land desertification. Notably, a significant proportion of farmland was transferred out in 1995 (Fig. 3 [FIGURE:3]). From 1990 to 2020, the largest area of conversion was desert, totaling 27,533.48 km^2, of which approximately 42.00% (11,650.20 km^2) was converted from bare land. Urban land, as well as water body, also increased by 9,341.04 and 1,737.81 km^2, respectively. These changes reflect the impacts of rapid urbanization and climate change on land use in the basin. The largest area transferred out was

bare land, reaching 14,370.83 km^2, likely due to factors such as soil erosion and urbanization (Table 5).

3.3 Spatial and Temporal Variations in Human Activity Intensity

Over the past 30 years, the equivalent area of urban land and the intensity of human activities in the Tuha Basin have shown a downward trend followed by an upward trend (Fig. 4a [FIGURE:4]). The urban land equivalent percentage in 1990 was 3.29%, and reached the lowest point in 2000. After 2000, the urban land equivalent percentage increased continuously, reaching 3.24% in 2020. The human activity intensity in 1990 was 4.32%, and reached its lowest point in 2010 with a value of 2.87%. After 2010, the human activity intensity increased rapidly, rising to 3.99% in 2020. However, from 1990 to 2020, the intensity of human activities in the basin was always lower than the national average due to the combined effects of the region' s remote geographic location, arid climate, and fragile ecological environment.

The intensity of human activities varied significantly between counties and districts in the Tuha Basin (Fig. 4b [FIGURE:4]). In Turpan City, the index for the three counties and districts (Shanshan County, Toksun County, and Gaochang District) followed a pattern of first increasing, then decreasing, and then increasing again, with 1995 and 2010 marking the transition points. In contrast, Yizhou District in Hami City showed a trend of first decreasing and then increasing, with 2015 serving as the boundary. The trends in Barkol Kazak Autonomous County and Yiwu County in Hami City were more complex. Among these areas, Gaochang District in Turpan City had the highest human activity intensity indices, all exceeding 4.98%. The index in this district was 5.99% in 1990, rose to 7.90% in 1995, dropped to 4.98% in 2010, and then rapidly increased to 8.42% in 2020. On the other hand, Shanshan County in Turpan City had the lowest human activity intensity indices, all below 2.63%. The index for this county was 1.78% in 1990, increased to 1.82% in 1995, decreased to 1.01% in 2010, and then rapidly increased to 2.63% in 2020.

To better understand the spatial differentiation of human activity intensity in the Tuha Basin, we calculated and categorized the intensity levels at the township scale into five levels: relatively low, low, medium, relatively high, and high, based on the grading criteria of 0.00%-5.00%, 5.00%-15.00%, 15.00%-30.00%, 30.00%-45.00%, and >45.00% (Fig. 5 [FIGURE:5]; Table S3). High-intensity areas were mainly clustered in the core urban townships of Gaochang District and Yizhou District. The number of zones with human activity intensity greater than 45.00% decreased from 1990 to 2010, but average intensity increased. By 2020, the number of high-intensity zones had risen to 12, with the new zones mainly composed of areas that had transitioned from medium to high intensity. From 1990 to 2020, the number of township-level units with higher-intensity zones increased, with the average intensity rising from 36.82% in 1990 to 38.13% in 2020. These zones were initially concentrated in densely populated counties

and municipalities (such as the southern edge of Barkol Kazak Autonomous County, north-central part of Yizhou District, and south-central to northern area of Gaochang District), but later expanded to include the northeastern corner of central Yizhou District and northwestern extremity of Shanshan County, which were transformed from medium-intensity zones. Some of these areas were also reclassified from high-intensity zones (e.g., north-central sector of Shanshan County) or low-intensity zones (e.g., eastern extremity of central Yizhou District). Medium-intensity zones are mainly located around the urban areas of Hami City and Turpan City, as well as the southern part of Barkol Kazak Autonomous County. Relatively low and low-intensity zones accounted for about 50.00% of the Tuha Basin. The numbers of these zones decreased from 62 in 1990 to 50 in 2020.

3.4 Spatial Autocorrelation of Human Activity Intensity

The intensity of human activities in the Tuha Basin over the past 30 years has been characterized by significant spatial clustering (Table S4). From 1990 to 2015, the Moran' s I index ranged from 0.46 to 0.68, indicating that there was no substantial change in the spatial aggregation of human activity intensity during this period. However, in 2020, the Moran' s I index rapidly increased to 0.91, reflecting a significant enhancement in the spatial aggregation of human activity intensity. This abrupt increase suggests a structural transformation in the spatial distribution of human activities, possibly driven by development strategy and policy, and land use agglomeration in recent years. To further examine these spatial differences, we identified the hot and cold spots of human activity intensity and their changes from a spatial correlation perspective (Fig. 6 [FIGURE:6]).

Over the past 30 years, the overall pattern of hot and cold spots of human activity intensity in the Tuha Basin has remained largely stable, though the proportions of different zones have changed over time. The range of cold spots at the 99.00% confidence level has disappeared and shifted to an intermediate state. The range of cold spots at the 95.00% confidence level has remained largely unchanged, while the range of cold spots at the 90.00% confidence level has expanded. As a result, the area covered by cold spots gradually increased from 2.26% in 1990 to 7.90% in 2020. The range of hot spots at the 99.00% confidence level fluctuated, decreasing from 1990 to 2000 and then increasing from 2000 to 2020. Hot spots at the 99.00% confidence level were primarily located in and around the city centers of Turpan and Hami. The range of hot spots at the 95.00% confidence level increased, while the extent of hot spots at the 90.00% confidence level decreased, with hot spots declining from 13.07% in 1990 to 9.24% in 2020. Overall, the aggregation effect of hot spots was weakening, while the aggregation effect of cold spots was strengthening. However, the cold-spot aggregation effect remained weaker than that of the hot spots, indicating that the spatial pattern of human activity in the Tuha Basin was shifting. The center of human activity has dispersed, with new areas gradually being incorporated

into regional exploitation, though the existing core areas continue to dominate.

3.5 Drivers of Changes in Human Activity Intensity

The factor detection revealed that topographic and geomorphological elements had the strongest explanatory power for the spatial pattern of human activity intensity in the Tuha Basin, while climatic and socio-economic factors showed relatively weaker explanatory power (Table 6). Among the topographic factors, slope had the strongest influence, with a q-value of 0.48, indicating that slope was the primary factor shaping human activity intensity in the basin. Areas with steeper slopes were less conducive to human activities, while flatter areas were more easily developed, leading to higher human activity intensity. Slope orientation (aspect) also played a significant role, with a q-value of 0.38. This result suggested that the orientation of slopes influenced human activities, as certain orientations, such as southern-facing slopes, received more sunlight and were more suitable for agricultural activities, which in turn led to higher human activity intensity in those areas. Precipitation, with a q-value of 0.11, showed weak explanatory power for human activity intensity. Although precipitation is important for agriculture, the basin experiences low precipitation, and agricultural activities primarily rely on irrigation. Finally, GDP had the weakest explanatory power, with a q-value of 0.05. This result was likely due to the economic structure and the type of human activities in the basin, which were not strongly tied to GDP fluctuations.

Geodetector interaction factor analysis showed that the q-values for two-factor interaction were higher than those for corresponding single-factor analysis, indicating a synergistic enhancement effect. This result suggests that when two or more factors act together, their combined impact on the spatial patterns of human activity intensity is much greater than the sum of their individual effects (Fig. 7

). Specifically, the interaction between slope and agricultural output had the highest explanatory power (q = 0.71), which indicated that slope, as a topographic factor, directly influenced land use patterns and the accessibility of areas for human activities, while agricultural output reflected the efficiency of agricultural production. The synergy of these two factors significantly enhances the spatial differentiation of human activity intensity in areas with specific slopes and high agricultural productivity. Moreover, the interaction between slope orientation and agricultural output also demonstrated strong explanatory power (q = 0.66). Slope orientation influenced human activities by affecting natural conditions such as sunlight, temperature, and precipitation, and its interaction with agricultural output further revealed the differentiated impacts of agricultural productivity on human activity intensity under varying slope conditions.

In summary, the spatial heterogeneity of human activity intensity in the Tuha Basin was mainly driven by topographic factors such as slope, aspect, and agricultural output, which had a significant enhancement effect under interaction

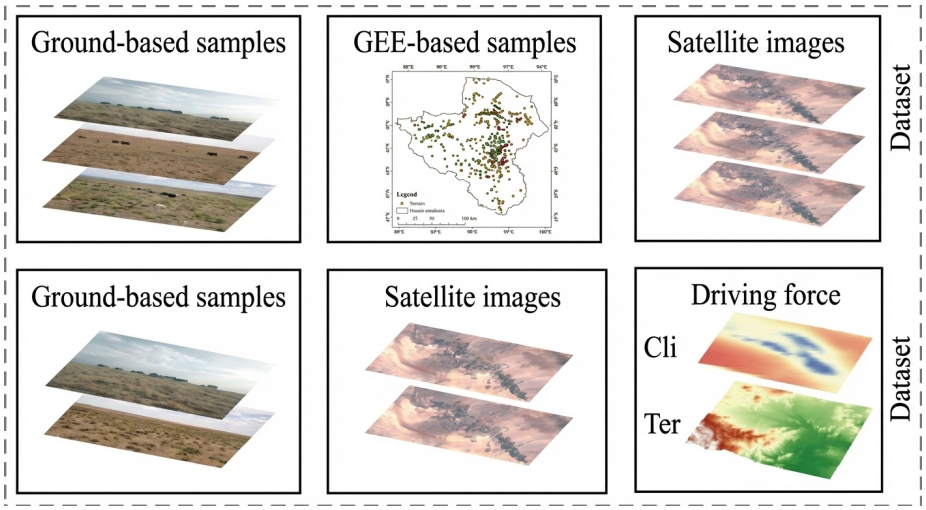

Figure 1: Figure 7

(Fig. 7). However, it must be deeply recognized that the extremely dry climate background (manifested by precipitation and temperature factors with low q-values) is the underlying decisive framework for shaping the basic spatial pattern of human activities (oasis distribution) and ecosystem carrying capacity in the basin. Its low single-factor explanatory power precisely highlights the fundamental status of water resources as a rigid constraint, the high sensitivity and vulnerability of ecosystems to climate change, and the long-term sustainability challenges inherent in human regulation while overcoming short-term constraints.

4.1 Land Use Validation

In this study, the reliability of the Tuha Basin land use dataset was assessed by systematically comparing it with the CLCD and GLC_{FCS30D} datasets. The dataset used in this study adopted a high spatial resolution of 30.00 m and provides annual time-series data from 1990 to 2020, enabling it to capture subtle land use changes in the basin. The classification process integrated field sampling and visual interpretation sample points, enhancing the credibility of the results [**?**]. The overall accuracy of this dataset was 0.82, slightly higher than that of the CLCD (0.79) [**?**] and GLC_{FCS30D} (0.81) [**?**].

Although the three datasets differed in certain land cover conversion details, such as inconsistencies in the conversion patterns of desert to urban, rural, or agricultural land, the overall conversion trends were broadly consistent. All datasets reflected a significant trend of desertification in the Tuha Basin (Table 7). This result not only demonstrated the reliability of the Tuha Basin dataset in identifying major land use changes but also highlighted its effectiveness in

capturing the intensity of human activities and ecological shifts in the basin. It is important to note that CLCD and GLC_{FCS30D} represent national and global scales, respectively, and their classification systems have some limitations in terms of regional adaptability. In contrast, the Tuha Basin dataset is specifically tailored to the basin, making it more relevant and effective in capturing regional details and reflecting local trends.

4.2 Spatial and Temporal Variations in the Intensity of Human Activities

A larger proportion of farmland was transferred out in 1995, which was closely related to the reform of the market economy in China, which accelerated in the mid-1990s. The restructuring of state-owned enterprises and the development of the coastal economy prompted rural labor to shift to non-agricultural industries. This transition led to reduced inputs for farmland management and the abandonment of marginal lands.

The intensity of human activities in the Tuha Basin decreased between 1990 and 2000, likely due to socio-economic factors, including population outmigration during that period [**?**]. However, with the promotion of the Western Development Strategy, infrastructure expansion, and the development of energy resources such as coal, oil, and gas [**?**], the intensity of human activities rebounded rapidly from 2010 to 2020. Despite this growth, the Tuha Basin' s human activity intensity remained lower than the national average due to its remote location, arid climate, and fragile ecological environment, highlighting the natural constraints on development in the basin [**?**, **?**].

Spatially, the distribution of human activity intensity in the Tuha Basin is closely tied to the topography and natural resource conditions [**?**]. High-intensity zones were primarily concentrated in the core areas of Yizhou and Gaochang districts, which featured flat terrain and abundant soil and water resources. This result underscored the influence of topography and water resources on population concentration [**?**, **?**]. Medium-intensity zones (15.00%–30.00%) surrounded urban areas, reflecting the "gradient effect" of urban expansion [**?**]. Low-intensity zones mostly occurred in ecologically fragile, high-elevation, or desert areas, further emphasizing the role of the natural geographic environment in shaping human activities [**?**].

Notably, the sharp rise in Moran' s I index to 0.91 in 2020 reflected a turning point in the spatial dynamics of human activities in the Tuha Basin. This abrupt increase may be attributed to several converging factors. First, the sustained implementation of the Western Development Strategy and the Belt and Road Initiative has intensified infrastructure investment and promoted spatially concentrated development, especially in transport corridors and energy bases [**?**, **?**]. Second, rural land consolidation and urban-rural integration policies have enhanced land use efficiency and driven the formation of contiguous high-intensity zones [**?**]. Third, ecological migration projects have relocated populations away

from ecologically fragile zones to urban peripheries or core towns, contributing to spatial polarization in human activity distribution [?]. Together, these development-oriented, ecological, and demographic transitions have accelerated the spatial clustering of human activity intensity in the basin in 2020, consistent with broader patterns of regional agglomeration in western China.

Over the past 30 years, the Moran' s I index of human activity intensity in the Tuha Basin has significantly increased, indicating a growing spatial aggregation of human activities. This trend is closely linked to the acceleration of regional economic development, urbanization, and infrastructure construction. Economic growth and urbanization have gradually concentrated populations and economic activities in key centers, enhancing spatial agglomeration [?]. Meanwhile, improved infrastructure has strengthened the connections between core and peripheral areas, further facilitating the spatial clustering of human activities [?].

In addition, the Tuha Basin, as an important energy base in China, has seen a significant increase in the development of its coal, oil, and natural gas resources in the last two decades, which has greatly contributed to the construction of regional infrastructures and the movement of population [?]. However, energy development activities are usually concentrated in desert or Gobi areas with fragile ecological environments [?], which are highly susceptible to irreversible perturbations of local fragile ecosystems. The increased spatial aggregation of human activity intensity also implies that the impacts of energy development on local ecosystems are intensifying. Therefore, the identification of spatial and temporal evolution of human activity intensity and its driving mechanisms in this study can help to clarify the key coordination zones between energy development and ecological protection, and thus provide a scientific basis and spatial reference for energy bases to achieve a balance between development and protection.

4.3 Factors Influencing Changes in the Intensity of Human Activities

Topographic factors, especially slope, aspect, and elevation, play a dominant role in shaping the distribution of human activity intensity in the Tuha Basin. Slope directly limits the scope and extent of developmental activities and indirectly influences the spatial pattern of human activities by affecting land use efficiency and accessibility [?]. Slope orientation also significantly impacts human activities, with southern slopes being more suitable for agricultural production due to their abundant sunlight [?], thus attracting more human activities. These topographic factors not only highlight the constraints and guidance of the natural environment on human activities but also reflect the process of mutual adaptation and optimization between human activities and the natural environment.

Although temperature and precipitation influence agricultural production and living conditions in the Tuha Basin, their direct explanatory power for the in-

tensity of human activities is relatively weak. However, climatic factors still play an important role in land use and development, especially in the context of sustainable development [**?**, **?**]. The Tuha Basin experiences an extremely arid climate, with an average annual precipitation of less than 20 mm and an annual evaporation rate of up to 3300 mm, an average annual temperature of 9.8°C, and extreme high temperatures reaching 48.0°C [**?**]. These harsh climatic conditions pose significant challenges to agricultural production and water resource utilization but also create a unique advantage in terms of light and heat resources. Additionally, climatic factors indirectly influence human activity patterns through the spatial distribution of water resources. For example, the basin depends on meltwater from the Tianshan Mountains. Although the oasis area comprises less than 3.00% of the total area, it hosts more than 80.00% of the population, creating a fragile ecological balance of "extreme drought-oasis dependence" [**?**].

Areas with higher agricultural output are generally associated with higher human activity intensity. According to the National Economic and Social Development Statistics Bulletin for Gaochang District in 2020, the gross value of agriculture, forestry, animal husbandry, and fishery in 2020 amounted to 4.04$×10^{9}$ CNY, a 4.40% increase from the previous year, while the intensity of human activities in 2020 was 8.42%, showing a 19.30% increase from the previous year. The booming agricultural development not only promotes the formation of related processing and logistics industries but also strengthens the industrial agglomeration effect. In the Tuha Basin, although the impact of population density on human activity intensity is limited, the impact still remains non-negligible. High population densities generally promote regional economic and social development; however, in areas with relatively low population densities, the direct effect of population on human activity intensity is less significant [**?**].

The results of the interaction detector indicate significant synergistic effects among driving factors, with all interaction q-values exceeding those of the corresponding single-factor detectors, reflecting the widespread presence of nonlinear enhancement mechanisms. Among them, the interaction between slope and agricultural output exhibited the highest explanatory power ($q = 0.71$), suggesting that the combination of natural and economic factors significantly amplifies the influence on human activity intensity within specific spatial units. This enhancement can be attributed to the fact that slope constrains the spatial boundary of arable land development, while agricultural output reflects the efficiency of human utilization of limited natural resources. The interaction between these two factors not only determines the location of high-potential agricultural zones but also shapes the spatial distribution pattern of human activity intensity. Similarly, the interaction between aspect and agricultural output ($q = 0.66$) reveals the spatial adaptability of agricultural production under varying topographic light and heat conditions. For instance, sun-facing slopes benefit from better solar radiation and thermal conditions, which can increase yield per unit area and enhance the attractiveness for human activities. This coupling effect be-

tween topography and economic factors reflects a complex feedback mechanism between natural resource conditions and human activities, where both sides mutually influence and constrain each other [**?**]. Moreover, although climate factors alone show relatively low explanatory power for human activity intensity, their interactions with topographic or economic factors often significantly enhance explanatory capacity. This result suggests that in extremely arid environments, human interventions, such as agricultural irrigation systems and land development policies, can partially compensate for climatic disadvantages, enabling the climatic constraints to be partially "overcome" in the context of factor interactions [**?**].

In summary, the intensity of human activities in the Tuha Basin results from the combined effects of several factors, including topography, climate, economy, and policy. The interaction among these factors provides much greater explanatory power for human activity intensity than any single factor alone, reflecting the complex relationship between human activities and the natural environment. Therefore, when making decisions about land use and development, it is essential to consider these factors in an integrated manner to achieve a harmonious and sustainable balance between human activities and the natural environment.

5 Conclusions

This study systematically revealed the spatial and temporal evolution of human activity intensity in the Tuha Basin over the past 30 years, which was characterized by a "decline followed by recovery" trend. The interaction between topographic factors (slope and slope direction) and economic activities was quantitatively identified as the dominant force driving the spatial pattern of human activity intensity ($q = 0.71$), which profoundly revealed the complex coupling mechanism of human-topography relationships in arid areas. Meanwhile, a high-precision and long time series (from 1990 to 2020) land use dataset was constructed, which provides a solid data foundation and methodological support for related research in arid areas. Based on the above findings, the following three recommendations are put forward: Firstly, optimizing the spatial development pattern, taking into account the coupling effect of topography and economic activities in the process of land use and energy development, prioritizing the intensive development of areas with gentle slopes and good light and heat conditions, and limiting the disturbing development of areas with high slopes and ecological fragility are necessary. Secondly, strengthening the ecology-development synergy under the "dual-carbon" goal is essential to promoting the ecological monitoring and low-carbon transformation of high-intensity human activity zones and energy development zones. Thirdly, the rigid constraints on water resources should be emphasized, the agricultural structure should be optimized, and water-saving technologies should be promoted, so as to ensure the stability and sustainable development of the oasis ecosystem.

Conflict of Interest: ZHANG Yuanming is an editorial board member of *Journal of Arid Land* and was not involved in the editorial review or the decision

to publish this article. All authors declare that there are no competing interests.

Acknowledgements: This study was supported by the Third Xinjiang Scientific Expedition Program (2022xjkk1205) and the National Natural Science Foundation of China (42377461).

Author Contributions: Conceptualization: YIN Yuanyuan, HUANG Jixia, YIN Benfeng; Formal analysis: SHI Qingqing; Writing - original draft preparation: SHI Qingqing; Writing - review and editing: YIN Yuanyuan, HUANG Jixia, YIN Benfeng, ZHANG Yuanming; Funding acquisition: YIN Benfeng, YIN Yuanyuan; Supervision: YIN Yuanyuan, HUANG Jixia, YIN Benfeng, YANG Ao, ZHANG Yuanming; Investigation: YIN Yuanyuan, HUANG Jixia, YIN Benfeng, YANG Ao. All authors approved the manuscript.

References

Alam A, BiBi K, Khatwani M K. 2024. Xinjiang a gateway to China belt and road initiative and regional connectivity. *Journal of Pakistan-China Studies (JPCS)*, 5(1): 38–51.

Bloom D E, Canning D, Malaney P N. 2000. *Population Dynamics and Economic Growth in Asia*. New York: Population Council.

Chen M X, Zhang H, Liu W D, et al. 2014. The global pattern of urbanization and economic growth: Evidence from the last three decades. *PLoS ONE*, 9(8): e103799, doi: 10.1371/journal.pone.0103799.

Chen Y Y, Zhang L, Yan M, et al. 2024. Spatiotemporal evolution and future simulation of land use/land cover in the Turpan-Hami Basin, China. *Journal of Arid Land*, 16(10): 1303–1326.

Cheng Y, Liu H, Chen D M, et al. 2022. Human activity intensity and its spatial-temporal evolution in China' s border areas. *Land*, 11(7): 1089–1107.

Deng B S, Halik W, Zhang Y P, et al. 2015. Suitable scale and stability analysis of Turpan Oasis. *Arid Zone Research*, 32(4): 797–803. (in Chinese)

Dou X Y, Guo H D, Zhang L, et al. 2023. Dynamic landscapes and the influence of human activities in the Yellow River Delta wetland region. *Science of the Total Environment*, 899: 166239, doi: 10.1016/j.scitotenv.2023.166239.

Ellis E C, Ramankutty N. 2008. Putting people in the map: Anthropogenic biomes of the world. *Frontiers in Ecology and the Environment*, 6(8): 439–447.

Eswaran H, Lal R, Reich P F. 2001. Land degradation: An overview. In: *Proceedings of the 2nd International Conference on Land Degradation and Desertification*. Khon Kaen, Thailand.

Fan J, Sun W, Zhou K, et al. 2012. Major function oriented zone: New method of spatial regulation for reshaping regional development pattern in China. *Chinese Geographical Science*, 22(2): 196–209.

Fatemi M, Rezaei-Moghaddam K, Karami E, et al. 2021. An integrated approach of Ecological Footprint (EF) and Analytical Hierarchy Process (AHP) in human ecology: A base for planning toward sustainability. *PLoS ONE*, 16(4): 0250167, doi: 10.1371/journal.pone.0250167.

Fu P D, Rich P M. 2002. A geometric solar radiation model with applications in agriculture and forestry. *Computers and Electronics in Agriculture*, 37(1): 25–35.

Gao Y, Bai L Y, Zhou K F, et al. 2024. Study on the coupling coordination degree and driving mechanism of "Production-Living-Ecological" space in ecologically fragile areas: A case study of the Turpan-Hami Basin. *Sustainability*, 16(20): 9054, doi: 10.3390/su16209054.

Hou Y F, Chen Y N, Li Z, et al. 2023. Changes in land use pattern and structure under the rapid urbanization of the Tarim River Basin. *Land*, 12(3): 693–710.

Intergovernmental Panel on Climate Change (IPCC). 2023. *Climate Change 2021-The Physical Science Basis: Working Group I Contribution to the Sixth Assessment Report of the Intergovernmental Panel on Climate Change* (1st ed.). Cambridge: Cambridge University Press.

Jiang Z J, Lin B Q. 2012. China' s energy demand and its characteristics in the industrialization and urbanization process. *Energy Policy*, 49: 608–615.

Karalas K, Tsagkatakis G, Zervakis M, et al. 2016. Land classification using remotely sensed data: Going multilabel. *IEEE Transactions on Geoscience and Remote Sensing*, 54(6): 3548–3563.

Li B F, Gui D W, Xue D P, et al. 2022. Analysis of the expansion characteristics and carrying capacity of oasis farmland in Northwestern China in recent 40 years. *Agronomy*, 12(10): 2448, doi: 10.3390/agronomy12102448.

Li S C, Wu J S, Gong J, et al. 2018. Human footprint in Tibet: Assessing the spatial layout and effectiveness of nature reserves. *Science of the Total Environment*, 621: 18–29.

Li S N, Zhu C M, Deng X D. 2024. Exploring the urban–rural gradient effects of construction land expansion processes on land use function trade-off/synergy in rapidly urbanizing areas. *Land Degradation & Development*, 35(1): 46–61.

Liang S J. 2020. Achievements and potential of petroleum exploration in Tuha Oil and Gas Province. *Xinjiang Petroleum Geology*, 41(6): 631–641. (in Chinese)

Liu H C, Fan J, Zhou K, et al. 2023. Assessing the dynamics of human activity intensity and its natural and socioeconomic determinants in Qinghai-Tibet Plateau. *Geography and Sustainability*, 4(4): 294–304.

Liu X B, Wang Y K, Li M. 2021. Theory, method and technological application of territorial spatial development suitability evaluation. *Journal of Geo-information Science*, 23(12): 2097–2110. (in Chinese).

Liu Y B, Chen Y N. 2006. Impact of population growth and land-use change on water resources and ecosystems of the arid Tarim River Basin in Western China. *International Journal of Sustainable Development & World Ecology*, 13(4): 295–305.

Ma R. 2015. The evolution of ethnic relations in China' s urbanization process. *Northwest Journal of Ethnology*, 1: 19–34. (in Chinese)

Mendelsohn R, Dinar A. 2009. Land use and climate change interactions. *Annual Review of Resource Economics*, 1: 309–332.

Moran P A P. 1948. The interpretation of statistical maps. *Journal of the Royal Statistical Society B*, 37: 243–251.

Moran P A P. 1950. Notes on continuous stochastic phenomena. *Biometrika*, 37: 17–33.

Mu H W, Li X C, Wen Y N, et al. 2022. A global record of annual terrestrial Human Footprint dataset from 2000 to 2018. *Scientific Data*, 9(1): 176–184.

Olofsson P, Foody G M, Herold M, et al. 2014. Good practices for estimating area and assessing accuracy of land change. *Remote Sensing of Environment*, 148: 42–57.

Ord J K, Getis A. 1955. Local spatial autocorrelation statistics: Distribution issues and an application. *Geographical Analysis*, 27(4): 286–306.

Riazi I. 2024. Urban-rural linkages: Improving regional development through enhanced connectivity. *Kashf Journal of Multidisciplinary Research*, 1(04): 19–26.

Sanderson E W, Jaiteh M, Levy M A, et al. 2002. The human footprint and the last of the wild. *BioScience*, 52(10): 891–904.

Shao W, Li L, Yan M, et al. 2024. Thirty years' spatio-temporal evolution of desertification degrees and driving factors in Turpan-Hami Basin, Xinjiang, China. *Ecological Indicators*, 166: 112484, doi: 10.1016/j.ecolind.2024.112484.

Stehman S V, Wickham J. 2020. A guide for evaluating and reporting map data quality: Affirming Shao et al. "Overselling overall map accuracy misinforms about research reliability" . *Landscape Ecology*, 35: 1263–1267.

Tan L Y, Guo G C, Li S C. 2022. The Sanjiangyuan Nature Reserve is partially effective in mitigating human pressures. *Land*, 11(1): 43–57.

Tan Y M, Liu W H, Huang W J, et al. 2024. Analysis of the changes in the intensity of human activities in China in the past 40 years and their driving forces. *Geographical Science Research*, 13(4): 700–711. (in Chinese)

Telbisz T, Bottlik Z, Mari L, et al. 2014. The impact of topography on social factors: A case study of Montenegro. *Journal of Mountain Science*, 11(1): 131–141.

Venter O, Sanderson E W, Magrach A, et al. 2016. Global terrestrial human footprint maps for 1993 and 2009. *Scientific Data*, 3: 160067, doi: 10.1038/sdata.2016.67.

Wang J F, Xu C D. 2017. Geodetector: Principle and prospective. *Acta Geographica Sinica*, 72(1): 116–134. (in Chinese)

Wang S, Fu B J, Zhao W W, et al. 2018. Structure, function, and dynamic mechanisms of coupled human–natural systems. *Current Opinion in Environmental Sustainability*, 33: 87–91.

Wang Y, Xia T T, Shataer R, et al. 2021. Analysis of characteristics and driving factors of land-use changes in the Tarim River Basin from 1990 to 2018. *Sustainability*, 13(18): 10263, doi: 10.3390/su131810263.

Wang Y, Shataer R, Zhang Z C, et al. 2022. Evaluation and analysis of influencing factors of ecosystem service value change in Xinjiang under different land use types. *Water*, 14(9): 1424, doi: 10.3390/w14091424.

Wu J W, Xiao J Y, Hou J M, et al. 2023. Development potential assessment for wind and photovoltaic power energy resources in the main Desert–Gobi–wilderness areas of China. *Energies*, 16(12): 4559, doi: 10.3390/en16124559.

Xu H Q. 2006. Modification of normalised difference water index (NDWI) to enhance open water features in remotely sensed imagery. *International Journal of Remote Sensing*, 27(14): 3025–3033.

Xu W, Rao S, Wang X L, et al. 2025. Characteristics of middle Jurassic overpressure and tight gas accumulation in Shengbei sub-sag, Tuha Basin, Xinjiang. *Geology in China*, 52(2): 650–664. (in Chinese)

Xu X R, Xu Y. 2017. Spatiotemporal variation analysis of human activity intensity in the Loess Plateau region. *Geographical Research*, 36(4): 661–672. (in Chinese)

Xu Y, Xu X R, Tang Q. 2016. Human activity intensity of land surface: Concept, methods and application in China. *Journal of Geographical Sciences*, 26(9): 1349–1361.

Xue X, Liao J, Hsing Y T, et al. 2015. Policies, land use, and water resource management in an arid oasis ecosystem. *Environmental Management*, 55(5): 1036–1051.

Yang J, Huang X. 2021. The 30 m annual land cover dataset and its dynamics in China from 1990 to 2019. *Earth System Science Data*, 13(8): 3907–3925.

Yang K Z. 2021. China' s western development strategy for modernization drive. *China Economist*, 16(3): 62–83. (in Chinese)

Yang R J, Meng W, Shu J M, et al. 2017. Ecological civilization construction for the saline industry in the Qaidam Basin. *Chinese Journal of Engineering Science*, 19(4): 48–53.

Yang Y T, Xu H, Wang J W, et al. 2021a. Integrating climate change factor into strategic environmental assessment in China. *Environmental Impact Assessment Review*, 89: 106585, doi: 10.1016/j.eiar.2021.106585.

Yang Y Y, Bao W K, Wang Y S, et al. 2021b. Measurement of urban-rural integration level and its spatial differentiation in China in the new century. *Habitat International*, 117: 102420, doi: 10.1016/j.habitatint.2021.102420.

Yerkenhazi A, Mamat K, Abulizi A, et al. 2025. Identification of production-living-ecological spatial conflicts and multi-scenario simulations in extreme arid areas. *Land*, 14(5): 1002, doi: 10.3390/land14051002.

Zha X Z M, Jia S F. 2024. Development-ecological protection conflicts and coordination at West Taijinel Salt Lake. *Water*, 16(15): 2139, doi: 10.3390/w16152139.

Zha Y, Gao J Q, Ni S. 2003. Use of normalized difference built-up index in automatically mapping urban areas from TM imagery. *International Journal of Remote Sensing*, 24(3): 583–594.

Zhang T, Sun Y X, Guan M, et al. 2022a. Human activity intensity in China under multi-factor interactions: Spatiotemporal characteristics and influencing factors. *Sustainability*, 14(5): 3113, doi: 10.3390/su14053113.

Zhang W, Zhou L, Zhang Y, et al. 2022b. Impacts of ecological migration on land use and vegetation restoration in arid zones. *Land*, 11(6): 891, doi: 10.3390/land11060891.

Zhang X, Zhao T T, Xu H, et al. 2024. GLC_{FCS30D}: The first global 30 m land-cover dynamics monitoring product with a fine classification system for the period from 1985 to 2022 generated using dense-time-series Landsat imagery and the continuous change-detection method. *Earth System Science Data*, 16(3): 1353–1381.

Zhao G, B Zheng J H, Wang L, et al. 2023. Study on planting suitability and planting structure optimization of fruit trees in Xinjiang. In: *The 11th International Conference on Agro-Geoinformatics*. New York: International Society of Agromatics.

Zhi D M, Li J Z, Chen X, et al. 2023. New fields, new types and resource potentials of oil-gas exploration in Tuha Basin. *Acta Petrolei Sinica*, 44(12): 2122–2140. (in Chinese)

Zhu G F, Qiu D D, Zhang Z X, et al. 2021. Land-use changes lead to a decrease in carbon storage in arid region, China. *Ecological Indicators*, 127: 107770, doi: 10.1016/j.ecolind.2021.107770.

Appendix

Fig. S1 Land use types of CLCD (a) and GLC-FCS30D (b) in 2020. CLCD, China Land Cover Dataset. GLC_{FCS30D} is the first global fine land cover dynamic product at a 30.00-m resolution.

Table S1 China Land Cover Dataset (CLCD) reclassification rules

CLCD_{class}	Reclassification	CLCD_{class}	Reclassification
Cropland	Farmland	Shrubland	Forest land
Grassland	Forest land	Water body	Water body
Sonw/Ice	Water body	Barren land	Desert
Impervious	Urban land	Wetland	Water body

Table S2 GLC-FCS30D reclassification rules

GLC-FCS30_{class}	Reclassification	GLC-FCS30_{class}	Reclassification
Rainfed cropland	Farmland	Herbaceous cover	Forest land
Tree or shrub cover (Orchard)	Farmland	Irrigated cropland	Farmland
Open evergreen broadleaved forest	Forest land	Lichens and mosses	Forest land
Sparse vegetation (fc$ 15.00 15.00 15.00 40.00 40.00 $40.00%)	Forest land	Impervious surfaces	Urban land
Open mixed leaf forest (broadleaved and needle-leaved)	Forest land	Bare area	Desert
Closed mixed leaf forest (broadleaved and needle-leaved)	Forest land	Consolidated bare areas	Desert
Shrubland	Forest land	Unconsolidated bare areas	Desert
Evergreen shrubland	Forest land	Water body	Water body
Deciduous shrubland	Forest land	Permanent ice and snow	Water body

Note: GLC_{FCS30D} is the first global fine land cover dynamic product at a 30.00-m resolution; fc is the percentage of canopy cover.

Table S3 Human activity intensity classification in the Turpan-Hami (Tuha) Basin from 1990 to 2020

Intensity Level	Range (%)	1990	1995	2000	2005	2010	2015	2020
Relatively low	0.00–5.00	-	-	-	-	-	-	-
Low	5.00–15.00	-	-	-	-	-	-	-
Moderate	15.00–30.00	-	-	-	-	-	-	-
Relatively high	30.00–45.00	-	-	-	-	-	-	-
High	>45.00	-	-	-	-	-	-	-

Table S4 Spatial autocorrelation of human activity intensity in the Tuha Basin

Index	1990	1995	2000	2005	2010	2015	2020
Moran' s I	-	-	-	-	-	-	-
Z score	-	-	-	-	-	-	-
P value	-	-	-	-	-	-	-

Figures

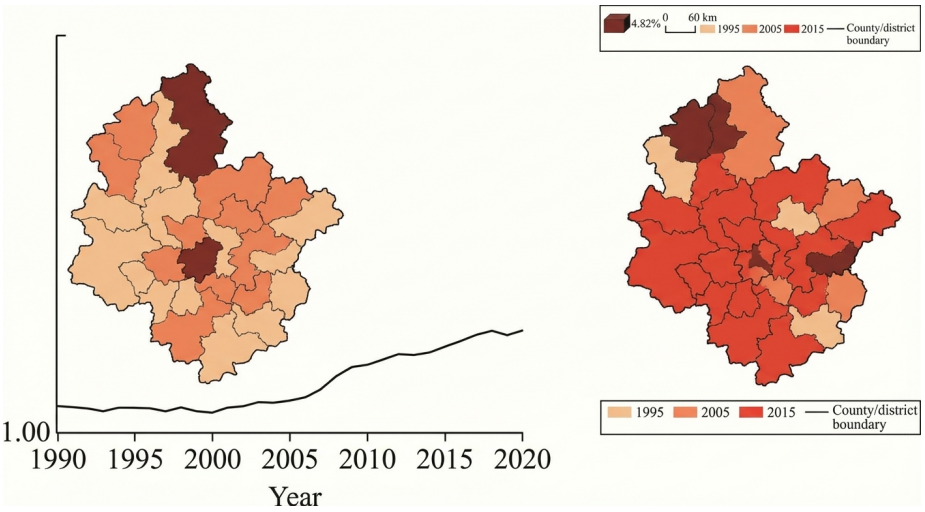

Figure 2: Figure 16

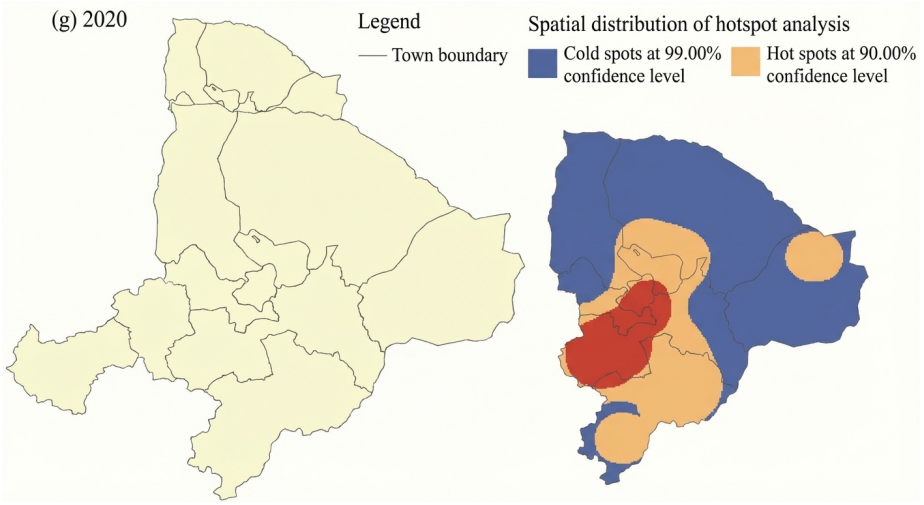

Figure 3: Figure 25

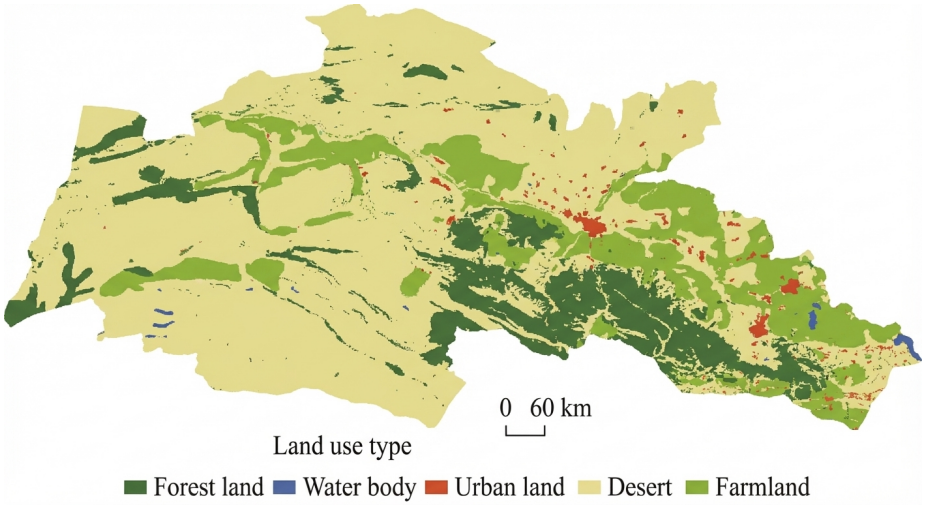

Figure 4: Figure 33